Journal of Applied Geophysics 112 (2015) 157–174

Contents lists available at ScienceDirect

Journal of Applied Geophysics

journal homepage: www.elsevier.com/locate/jappgeo

VES/TEM 1D joint inversion by using Controlled Random Search (CRS) algorithm

Cassiano Antonio Bortolozo [a,*], Jorge Luís Porsani [a], Fernando Acácio Monteiro dos Santos [b], Emerson Rodrigo Almeida [a]

[a] Universidade de São Paulo (USP), Instituto de Astronomia, Geofísica e Ciências Atmosféricas (IAG), Departamento de Geofísica, Rua do Matão, 1226, Butantã 05508-090, São Paulo, Brazil
[b] Instituto Don Luiz (IDL), Faculdade de Ciências, Universidade de Lisboa, 1749-016 Lisboa, Portugal

ARTICLE INFO

Article history:
Received 14 November 2013
Accepted 19 November 2014
Available online 28 November 2014

Keywords:
VES
TEM
1D joint inversion
Controlled Random Search (CRS)
Hydrogeology
Paraná Basin, Brazil

ABSTRACT

Electrical (DC) and Transient Electromagnetic (TEM) soundings are used in a great number of environmental, hydrological, and mining exploration studies. Usually, data interpretation is accomplished by individual 1D models resulting often in ambiguous models. This fact can be explained by the way as the two different methodologies sample the medium beneath surface. Vertical Electrical Sounding (VES) is good in marking resistive structures, while Transient Electromagnetic sounding (TEM) is very sensitive to conductive structures. Another difference is VES is better to detect shallow structures, while TEM soundings can reach deeper layers. A Matlab program for 1D joint inversion of VES and TEM soundings was developed aiming at exploring the best of both methods. The program uses CRS – Controlled Random Search – algorithm for both single and 1D joint inversions. Usually inversion programs use Marquadt type algorithms but for electrical and electromagnetic methods, these algorithms may find a local minimum or not converge. Initially, the algorithm was tested with synthetic data, and then it was used to invert experimental data from two places in Paraná sedimentary basin (Bebedouro and Pirassununga cities), both located in São Paulo State, Brazil. Geoelectric model obtained from VES and TEM data 1D joint inversion is similar to the real geological condition, and ambiguities were minimized. Results with synthetic and real data show that 1D VES/TEM joint inversion better recovers simulated models and shows a great potential in geological studies, especially in hydrogeological studies.

1. Introduction

Interpretation process ambiguities are always present in all kind of geophysical exploration. A way to reduce them consists in using different geophysical methods for the same problem. With a large and diverse database, ambiguities can be reduced, and the result becomes more trustful and close to reality. The challenge consists in the acquisition of different data sets related to subsurface physical proprieties from different geophysical methods. Data can be related to the same physical property or to some different properties. If the information is regarding the same physical property, data processing and interpretation are faster and simpler. Two methods exploring the same physical property in different manners are electrical and electromagnetic methods. Vertical Electrical Soundings (VES) and Transient Electromagnetic Soundings (TEM) explore vertical and lateral variations of resistivity in the underground. It is possible to make a simple approximation of underground for both methods in which subsurface has horizontal and isotropic layers with associated resistivity and thickness transforming these methods in ideal ones for a combined use.

Electrical methods (DC) are widely used in geophysics. The applications of these methods range from geotechnical, through mining, hydrogeological and environmental studies. They are widely used due its relatively low cost, velocity and survey reliability. Electromagnetic surveys are also widespread in mineral exploration, geotechnical engineering, and hydrogeology. Electromagnetic surveys can be divided into electromagnetic methods in frequency (FDEM), and time (TEM) domains. TEM has great potential in many applications, mainly in hydrogeological studies, and similar to geophysical methods, it has advantages and limitations. In Brazil, TEM method use is now increasing and some works are done in hydrogeological studies (Bortolozo et al., 2014; Carrasquila and Ulugergerli, 2006; Porsani et al., 2012a,b).

Time-Domain Electromagnetic method can accurately mark conductive structures and it has a great depth of investigation, in relation to the size of the loop used. In turn, Vertical Electrical Sounding method defines resistive structures very well, and can detect the most superficial subsoil layers. In this way, VES and TEM methods complement each other. However, the difference between how it obtains apparent resistivity curves makes the joint analyses complicated. In VES case, the

* Corresponding author at: Avenida Escola Politécnica, 2200, Ap. 42G - Bairro Rio Pequeno - São Paulo - SP CEP: 05350-000. Phone: +55 11 30912790 Cel: +55 11 976826063.
E-mail addresses: cassianoab@gmail.com, cassianoab@gmail.com (C.A. Bortolozo), porsani@iag.usp.br (J.L. Porsani), fasantos@fc.ul.pt (F.A.M. Santos), emerson1983era@gmail.com (E.R. Almeida).

http://dx.doi.org/10.1016/j.jappgeo.2014.11.014
0926-9851/

apparent resistivity curve is measure varying the electrode opening. In TEM sounding, apparent resistivity curve is measure as a function of medium time response. Therefore, apparent resistivity curve is in function of meters (AB spacing) in VES, and in TEM sounding, the apparent resistivity is in function of seconds. Then, analyses must be done by an inversion algorithm in order to deal with both databases, simultaneously.

With the aim of analyzing TEM and VES data more accurately and reliably the two-database joint inversion is necessary. In such case, it simultaneously does TEM and VES data inversion. Vozoff and Jupp (1975) assigned pioneering works related to the joint inversion of magnetotelluric data (MT) and Vertical Electrical Sounding (VES). In that article, authors showed the advantages of joint inversion, demonstrating how this process is synergistic, i.e., the final result is more than the sum of individual results of both methods. In this line of research, some studies have discussed the advantages of DC and TEM data joint inversion (Meju, 1996; Raiche et al., 1985; Yang and Tong, 1999), all showing the advantages of two-methodology joint use. Goldman et al. (1994) and Albouy et al. (2001) have applied the joint inversion of those methods in hydrogeological studies. Examples of application to potential risk of slopes are in Schmutz et al. (2000) and Schmutz et al. (2009).

Most of times, the inversion programs use a Marquadt type algorithm, which employs derivatives to find the global minimum. The problem in using this kind of algorithm for electric and electromagnetic methods is these methods have many local minimums, and the process may stop in a local minimum, leading to an erroneous model. In Monteiro Santos and El-Kaliouby's (2010) work, the authors compared derivative methods with global search methods for 1D joint inversion of VES/TEM, and they established the best ones for this case were global search ones.

A global search algorithm tries to find the objective function global minimum by searching the solution normally by a random search. The simplest approach would be to test all possible models but this would be impractical, even with the few amount of parameters normally used in 1D inversions. To overcome this problem, the search uses in many different ways random elements to map and find the global minimum of the objective function. Methods that incorporate random models inside algorithm are called Monte-Carlo methods (Mosegaard and Sambridge, 2002).

By using random models, it is possible to search objective function minimums faster than using systematic research (Mosegaard and Tarantola, 1995). However, simply testing a large number of random models without any control will be computationally expensive. To speed up the search, different techniques are developed to narrow the random search, it is worth to mention, among them: Simulated Annealing algorithm (Sen and Stoffa, 1991), neighborhood algorithm (Sambridge, 1999a,b), and genetic algorithms (Goldberg, 1989). CRS – Controlled Random Search – algorithm developed by Price (1977) is an algorithm that uses random models in a controlled form to be more efficient than only search random models but, also, robust enough to not fall in a local minimum. CRS was designed for thoroughness of search rather than for speed of convergence (Price, 1977), so it is not as fast as most of derivative methods but has at most a minimum chance to stop in a local minimum.

Since its development, CRS algorithm is worldly used in different kinds of applications. In Kim et al. (2005) work, they used CRS algorithm to determining the near-optimal settings of welding process parameters. The algorithm was also used for optimizing regression models (Křivý and Tvrdík, 1995; Křivý et al., 2000). In Merad et al. (2006), the authors formulated an optimization problem for designing nonuniformly spaced linear antenna arrays by using CRS algorithm. In geophysics, the use of CRS algorithm was especially in seismic, magnetic and magnetotelluric problems. Červ et al. (2007) used CRS algorithm to invert magnetotelluric data, obtaining good results. Smith and Ferguson (2000) demonstrated the benefits of CRS use when working with seismic refraction data, especially when focused on specific target investigation, CRS method proved highly effective at quantifying the statistics of the models. Silva and Hohmann (1983) used CRS for magnetic interpretation, concluding the algorithm is very robust, and, for the magnetic case, it can generate great results especially when geologic and geophysical information is available. All works involving the algorithm demonstrate the random search algorithms perform very well and are robust as they give great parameter determination for ill-structured global optimization problems.

In this article, we present a new approach to VES and TEM sounding 1D joint inversion the problem by using CRS algorithm, by the development and implementation of a program and the use of this methodology in southeastern Brazil. Joint inversion results are compared with results of individual inversions aiming at analyzing the advantage of 1D joint inversion. Therefore, this research may be of interest mainly for its application in hydrogeological studies, with emphasis on mapping fractured and sedimentary aquifers in tropical soils, for instance, at Paraná sedimentary basin.

2. Numerical modeling and inversion algorithm

The first step in the development of an inversion algorithm is the computation of the forward problem, which consists in our case in VES/TEM sounding numerical modeling. For VES, the code was developed based on Johansen (1975) by using linear filters to obtain the apparent resistivity. For TEM sounding (central loop), the program was developed using the filters developed by Christensen (1990) in the same form as Nielsen and Baumgartner (2006). CRS – Controlled Random Search – algorithm, developed by Price (1977) for global optimization was used in inversion. This algorithm is very adequate for our problem. The algorithm is very robust and a global inversion algorithm is the most indicate for VES/TEM data 1D joint inversion, as demonstrated by Monteiro Santos and El-Kaliouby (2010).

2.1. VES modeling

The method of linear filtering applied to electrical methods was developed by Ghosh (1971a,b). This method allows calculating the apparent resistivity with little computational cost, essential for a useful code. This method is consisting in solving the resistivity function integral by a convolution. The resistivity transform function is convolved with a set of previously calculated filters, and the result of this convolution is the apparent resistivity. Johansen (1975) improves the technique by using a longer set of filters, and it greatly increased the calculation accuracy. Thus, Johansen's formulation was used in this work.

Then, the apparent resistivity at the sampling points ($x_i = i\Delta x$) is given by:

$$\rho_a(i\Delta x) \sim \sum_{j=j_{min}}^{j_{max}} T((i-j)\Delta x + S)C(j\Delta x - S) \tag{1}$$

where T is the resistivity transform function; and C is the filter coefficients. In such a case, j_{min} and j_{max} are chosen, so that the filter coefficients with smaller or larger ratios may be neglected. S is a displacement factor calculated as demonstrated in Koefoed (1972) and Johansen (1975).

Resistivity transform for a stratified medium (Fig. 1a) can be calculated recursively (Koefoed, 1970). For a geoelectric layer above basement, the transform can be computed by using exponential formulation as:

$$T_{N-1}(\lambda) = \rho_{N-1}\frac{1-k_{N-1}e^{-2h_{N-1}\lambda}}{1+k_{N-1}e^{-2h_{N-1}\lambda}} \tag{2}$$

$$k_{N-1} = \frac{(\rho_{N-1}-\rho_N)}{(\rho_{N-1}+\rho_N)}. \tag{3}$$

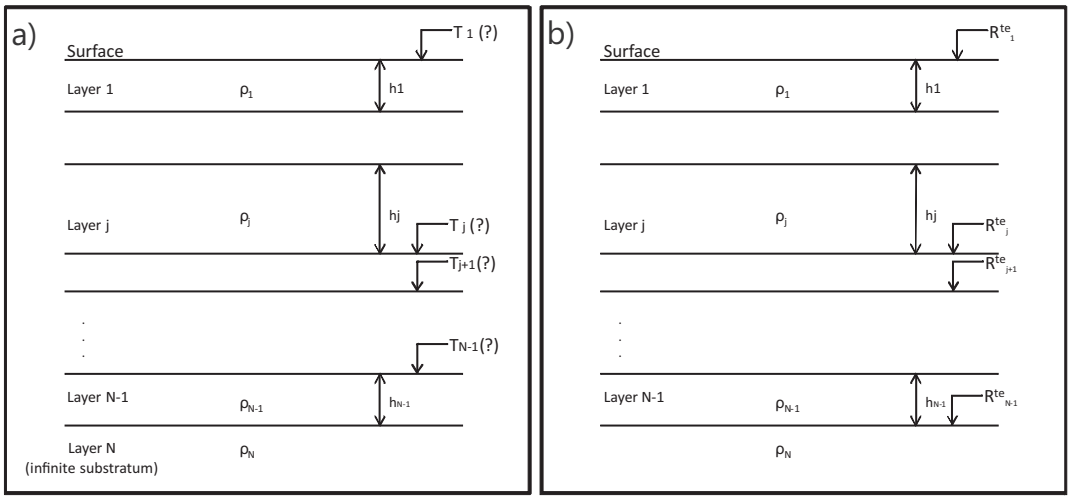

Fig. 1. a) Representation of resistivity transform T for a stratified earth with N layers. b) Representation of R^{TE} function for a stratified earth with N layers.

Transform T_j (ρ_j, h_j) at the top of the sequence of layers (ρ_{j+1}, ..., ρ_N; h_{j+1}, ..., h_{N-1}) is given by:

$$T_j(\lambda) = \frac{W_j(\lambda) + T_{j+1}(\lambda)}{1 + W_j(\lambda)T_{j+1}(\lambda)/\rho_j{}^2} \tag{4}$$

where

$$W_j(\lambda) = \rho_j \frac{1-e^{-2h_j\lambda}}{1+e^{-2h_j\lambda}} \tag{5}$$

and

$$j = N-2,\ N-3, \cdots,\ 2,\ 1 \tag{6}$$

by the recursive operation and considering $T_N = \rho_N$, we came to surface where $T = T_1(\lambda)$.

In having calculated resistivity transform, the next step is to calculate the convolution with filters. Apparent resistivity can be calculated as follows:

$$\rho_a(i) \approx \rho_N C_*^{j_1} + \sum_{j_1+1}^{j_2-1} T^{(i-j)} C^{(j)} + \rho_1 C_*^{j_2} \tag{7}$$

where

$$C_*^{j_1} = \sum_{j=-\infty}^{j_1} C^{(j)} \text{ and } C_*^{j_2} = \sum_{j=j_2}^{\infty} C^{(j)}. \tag{8}$$

In Johansen's (1975) case, the filter boundaries were defined as $j_1 = -100$ and $j_2 = 40$ (141 coefficients). The coefficients $C_*^{j_1}$ and $C_*^{j_2}$ are the minimum and maximum filter values, previously calculated in Johansen (1975). Calculation accuracy for this filter is in the order of 10^{-3}, very adequate to our needs.

2.2. TEM modeling

Similarly to the Vertical Electrical Sounding, the solution for TEM modeling is calculated by linear filtering. In Nielsen and Baumgartner (2006), the authors present the equation to calculate the magnetic field above a horizontally stratified earth assuming the loop is on the surface ($z = 0$). Magnetic field at the center of the loop is expressed by:

$$H_z(\omega) = aI \cdot \int_0^{\infty} \left[\frac{2R_1^{TE} u_1 \lambda}{R_1^{TE}(k_1^2 - k_0^2) + (u_0 - u_1)^2} - \frac{1}{2} \right] J_1(\lambda a)\lambda d\lambda + \frac{I}{2a} + \\ + \frac{I}{(k_1^2 - k_0^2)a^3} \left(\left(k_0^2 a^2 - 3ik_0 a - 3 \right) e^{-ik_0 a} - \left(k_1^2 a^2 - 3ik_1 a - 3 \right) e^{-ik_1 a} \right). \tag{9}$$

At sufficiently low frequencies $k_0 \approx 0$, the Eq. (10) can be simplified as:

$$H_z(\omega) = aI \cdot \int_0^{\infty} \left[\frac{2R_1^{TE} u_1 \lambda}{R_1^{TE} k_1^2 + (\lambda + u_1)^2} - \frac{1}{2} \right] J_1(\lambda a)\lambda d\lambda + \frac{I}{2a} \\ - \frac{I}{k_1^2 a^3} \left(3 + \left(k_1^2 a^2 - 3ik_1 a - 3 \right) e^{-ik_1 a} \right) \tag{10}$$

The function R_1^{TE} is obtained by a recursive relation:

$$R_n^{TE} = \frac{R_{n+1}^{TE} + \psi_{n+1}^{TE}}{R_{n+1}^{TE}\psi_{n+1}^{TE} + 1} e^{-2u_n h_n} \tag{11}$$

$$\psi_{n+1}^{TE} = \frac{\frac{u_n}{\hat{z}_n} - \frac{u_{n+1}}{\hat{z}_{n+1}}}{\frac{u_n}{\hat{z}_n} + \frac{u_{n+1}}{\hat{z}_{n+1}}} \tag{12}$$

$$\hat{z}_n = i\omega\mu_n \tag{13}$$

$$k_n^2 = \omega^2 \varepsilon_n \mu_n - i\omega\mu_n\sigma_n \tag{14}$$

$$u_n = \sqrt{\lambda^2 - k_n^2} \tag{15}$$

and

$$R_N^{TE} = 0 \tag{16}$$

where h_n is the thickness of the layer; n. R^{TE} roles similar to resistivity transform in electrical survey case, as can be seen in Fig. 1b. I is the

current in the loop; a is the radius of circular loop, J_1 is Bessel function of order 1, and λ is the variable of integration.

Once the transient response is a causal function ($h_z(t) = 0$ for $t \leq 0$), the transformation of response from the frequency domain to time domain can be obtained in form of a *sine* or *cosine* transform (Nielsen and Baumgartner, 2006):

$$h_z(t) = -\frac{2}{\pi}\int_0^\infty \frac{1}{\omega} Im[H_z(\omega)]\cos(\omega t)d\omega \tag{17}$$

in Eq. (17) a step-current excitation was assumed.

The mutual impedance can be expressed as:

$$Z(\tau) = -\frac{2nb^2}{\sigma_1 a^3}\int_0^\infty Im\left[H_z\left(\frac{2g}{\sigma_1\mu_0 a^2}\right)\frac{2a}{I}\right] sine(g\tau)dg \tag{18}$$

where σ_1 is the conductivity of the first layer; $\tau = 2t(\sigma_1\mu_0 a^2)^{-1}$; $g = \frac{1}{2}\sigma_1\mu_0\omega a^2$; b is the receiver loop radius, and n is the number of turns.

In TEM case, there are two integrals to be calculated: the integral in (Eq. (10)), and the integral in (Eq. (18)). Firstly, we must obtain the integrand of (18), which is the magnetic field in the frequency domain (Eq. (10)). Both integrals are calculated by using the filter set developed by Christensen (1990). Once we have the mutual impedance, the apparent resistivity can be calculated in a simple way:

$$\rho_a(i) = \left[\frac{\sqrt{\pi}a^2 nb^2}{20Z(i)}\right]^{2/3}\left(\frac{\mu_0}{t(i)}\right)^{5/3} \tag{19}$$

2.3. Data inversion

Most geophysical inverse problems fit into the category of nonlinear problems, which include inversion of data collected with electrical and electromagnetic methods as Vertical Electrical Sounding and TEM survey. There are many algorithms for nonlinear data inversion but this type of inversion is complex and always requires a detailed study of its operation. Some methods use derivatives and others use global random search. In Monteiro Santos and El-Kaliouby (2010) work, the authors tested some inversion algorithms for VES/TEM data 1D joint inversion. The study concludes global random search algorithms generate the best results. In the paper, the advantages of global random search algorithms are presented, in which an initial model neither is needed nor needs to be relatively close to the solution as in derivatives methods. These characteristics are particularly important when dealing with joint inversion of different data sets. Good initial models (close to global minimum) for local inversion algorithms can be very difficult to obtain and only reached after several inversion trials. Based on these results, in here we apply a global random search algorithm called CRS – *Controlled Random Search* – developed by Price (1977).

Although CRS was not one of the algorithms used in Monteiro Santos and El-Kaliouby (2010), it is a robust algorithm, well suited for problems as the one investigated in this study (VES/TEM). Indeed, CRS is not a fast search method but has great ability to find global minimum and it is very stable. This algorithm was used to do single VES/TEM sounding inversions and used in VES/TEM data 1D joint inversion, since the structure of inversion remains practically the same. The change in 1D joint inversion is the objective function.

The objective function is an important aspect of inversion problem that must carefully be defined in order to obtain better results. In this work, we used quadratic objective functions for both, individual and joint inversions. For individual inversion of methods, we use the following objective function:

$$\phi\left(\tilde{d}, \boldsymbol{p}\right) = \left\|\tilde{d} - h(\boldsymbol{p})\right\| \tag{20}$$

where $\tilde{d}$ is the data and $h(\boldsymbol{p})$ the physical response of $\boldsymbol{p}$ model. As can be seen, there is no weighting in the objective function or regularization term. Thus, the inversion is not constrained. Our experience with CRS for DC and TEM methods showed that this type of function is very suitable for these methods.

In 1D joint inversion, the objective function incorporates terms of electrical survey and TEM survey as follows:

$$\phi_{Joint}\left(\tilde{d}, \boldsymbol{p}\right) = \alpha\left\|\tilde{d}_{VES} - h_{VES}(\boldsymbol{p})\right\| + \beta\left\|\tilde{d}_{TEM} - h_{TEM}(\boldsymbol{p})\right\| \tag{21}$$

where $\tilde{d}_{VES}$ is the electric survey data, $\tilde{d}_{TEM}$ is TEM survey data, $h_{VES}(\boldsymbol{p})$ and $h_{TEM}(\boldsymbol{p})$ are the calculated response for VES and TEM survey, respectively. α and β are weighting coefficients for both methods. At the beginning of the research, the idea was to consider giving more weight to electrical surveys corresponding to the shallow layers, and more weight to TEM associated to deeper layers. Nevertheless, a further situation analysis showed that weighting in our case was not necessary, and results fit both data sets. It demonstrates that, in here, good shallow VES resolution and the great TEM investigation depth were automatically pondered in the joint inversion.

As will be seen forward, TEM method cannot solve structures located until depths of about 10% the size of the current loop. It means that, in a survey using a square loop of 100 m of side, structures up to a depth of 10 m are not well defined. In the VES, shallow layers are well marked in data acquired from the first AB/2 positions. Since the depth of investigation is most limited by the size of the array, it is currently accepted that the maximum depth of investigation is about a quarter of the total current electrode distance, i.e., AB/4. However, in tropical areas, like in Brazil, where soils are very conductive the depths of investigation tend to be considerably smaller.

In our case, it is expected that the nature of inversion process balances the depth of investigation of each method. Once the electrical sounding is not going to be sensitive to layers below AB/4, characteristics of these layers will not influence VES resistivity curve. The same happens with TEM regarding shallow layers. When the method is not very sensitive to some structure, it does not induce error, it simple stands neutral to changes in the model. In such a way, when one of the methods is sensitive to some structures that does not happen with the other, all the information from that layer came from the sensitive one. Thus, there is a natural weighting of inverse problem. Imposing a weighting may disrupt this natural feature of the problem, leading to distorted solutions in somehow. Notwithstanding, in some cases weighting the method may be used but until now we did not use this feature in our inversions.

The basic operation of algorithm is found in Fig. 2. Initially it should be defined the total number of parameters n to be inverted. In this case, n parameters related to geoelectric parameters of model (layer resistivity and thickness). In the next step, we define an initial search space where obtains m random models. The value of m is typically given in the form of 7 n but a different value may be set for each problem. A larger value of m improve the coverage of the search space but at the same time make the convergence slower, once all models need to be updated for the whole problem be minimized. These m models are the set of models that will modify during the iterative part. Physical response of each model is calculated (forward calculation) for all m models as well the value of objective function for each one. These processes consist in the initial algorithm stage. Then the iterative part may start, in which it obtained every iteration P model by average of n models randomly select among m set of models. Then, another model is randomly select from m set (this model is not one of the n previously selected), and an average between P model and this $n + 1$ model is done. Having this resulting model T, its objective function is calculated. If the value of objective function of model T is larger than the highest one among m models, model T is discarded and iterative process continues. If the objective function is smaller than the highest one among m models, model

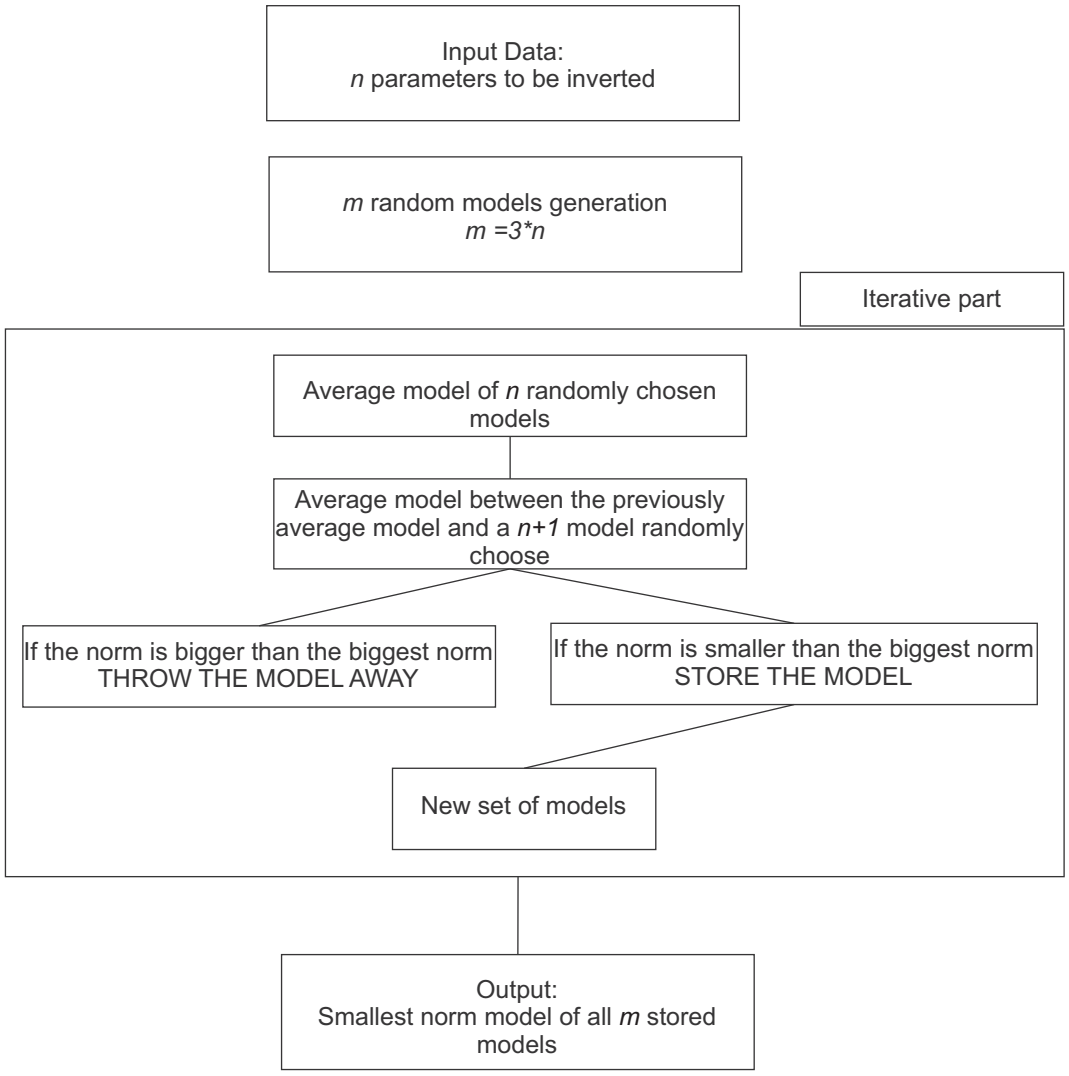

Fig. 2. Flowchart of CRS algorithm used in this work.

T enters in place of the model with the highest one, and iterative process continues. At the end of the process (which can be determined by a number of iterations or by the value of objective functions), there will be a set of models which ideally fit the data. The final model is that one with the lowest objective function. It can also make a representation of all final models. The probability that all models obtained converge to global minimum it will depend on the value of *n*, the complexity of objective function and initial search space.

One of the resulting graphics is all final models plotted together, and in an ideal result all models may have a minimal divergence, because after searching for whole space the best-selected models must be around global minimum. During iterative part, in CRS algorithm, selected models may fall in local minimums but also they eventually fall in global minimum. During selection of models, the ones in global minimum will have a lower RMS, and in this process, the algorithm with enough iterations selects only models in global minimum. This is the major advantage using global search algorithms. The use of some statistics for final models may lead to erroneous analyses because the idea is the search is tendentious for global minimum.

Normally for a single or joint inversion, some thousands of iterations are necessary, with a forward calculation for each iteration. For VES single inversion, it takes no more than 1 or 2 min. For TEM or joint inversion, this may take 10 to 20 min. This time is well acceptable, and, with modern computers, the program may run faster. In addition, a time around 10 min is well acceptable with irrelevant disadvantages compared with derivatives methods, once results have a minimal chance to stop in a local minimum.

Another feature of inversion program developed in this research is that one related to the "guessing" of initial search space. CRS needs, as a start, the number of parameters to be inverted and the interval of search (initial search space) for initial set of models. Initial search space corresponds to initial space where CRS algorithm will search for initial *m* random models used in the optimization. However, for operator's convenience the entrance of initial search space in developed program is done by the definition of initial search space midpoint. Initial search space in the algorithm goes from 10% of parameter entrance value to 190% of entrance value. Hence, in here "initial model" correspond to this initial search space midpoint. In the developed program, this search space restriction only occurs in the first part (initial model definition), the iterative algorithm part has no restrictions related to search space. The program is free to search the solution in the whole search space. Additionally, initial search space does not need to be close to the solution, even initial search space does not need to contain the solution, once there are any constrains in iterative part.

In Fig. 3 how the algorithm works is exemplified with two-variable case. In this example, by using VES, the simulated medium has two layers. The first one (to be determined) has a resistivity of 30 Ω.m and a thickness of 20 m. The second is geoelectric basement with 500 Ω.m.

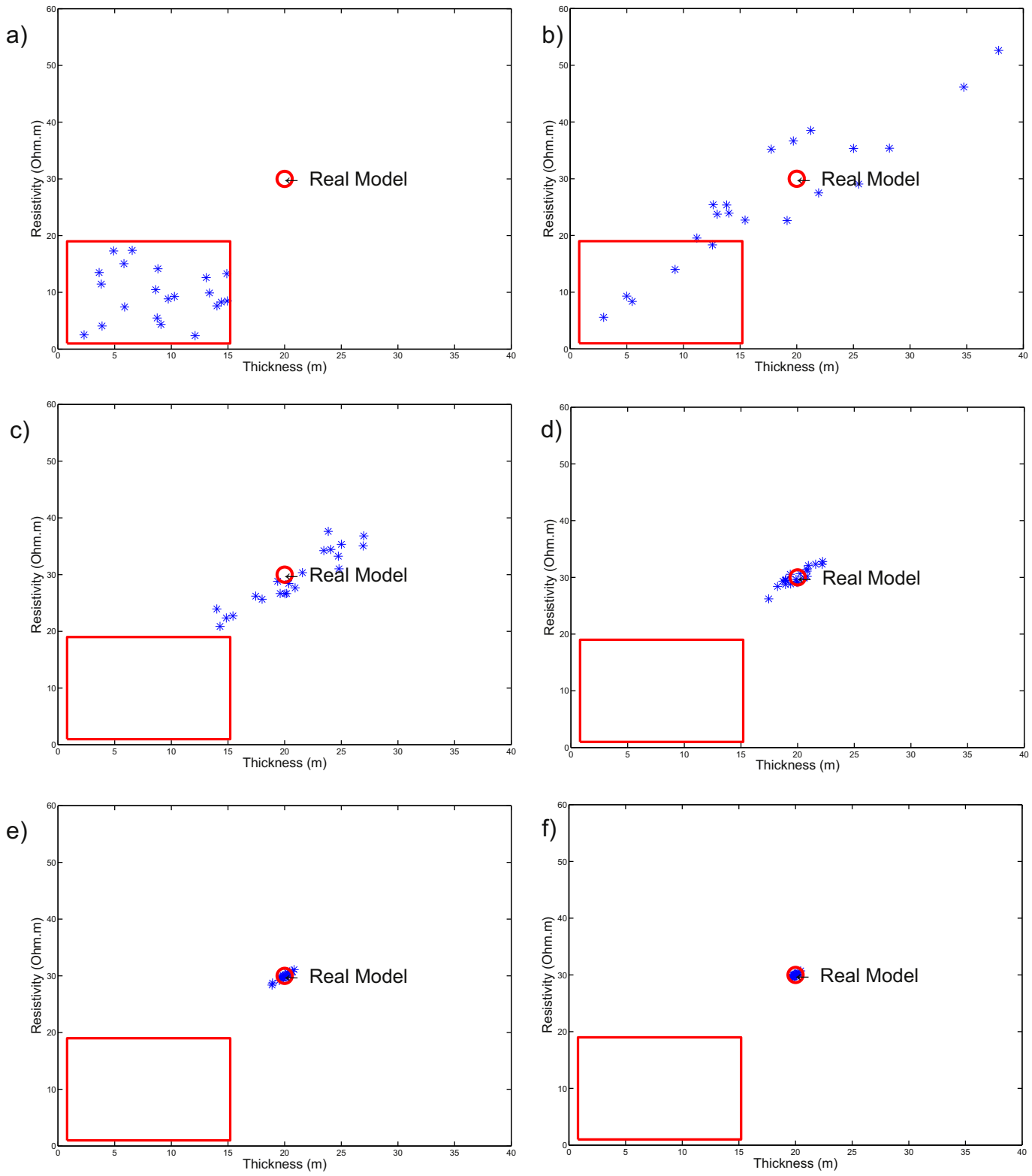

Fig. 3. An example of the way implemented algorithm works. Blue marks are models used in CRS algorithm; red box, the initial search space, and red circle, where the real (synthetic) model is. In a) initial randomly-determined models in initial search space. In b), c), d) and e) models in iterations 50, 100, 150, and 200 respectively. Finals models obtained by inversion are represented in f). (For interpretation of the references to color in this figure legend, the reader is referred to the web version of this article.)

In this example, the basement resistivity was constant and only first-layer variables were inverted. This example was developed for a better visualization of how CRS algorithm implemented in this research works. Fig. 3 shows models used in set of CRS algorithm models and how models chance during the iteration algorithm part. The red box in the figures is the representation of initial search space described above. Fig. 3a presents models obtained in the first algorithm step where all models are randomly selected in initial search space. In this case, the solution is not contained in this initial search space. Then, to reach the real values, the algorithm must be free to leave the red

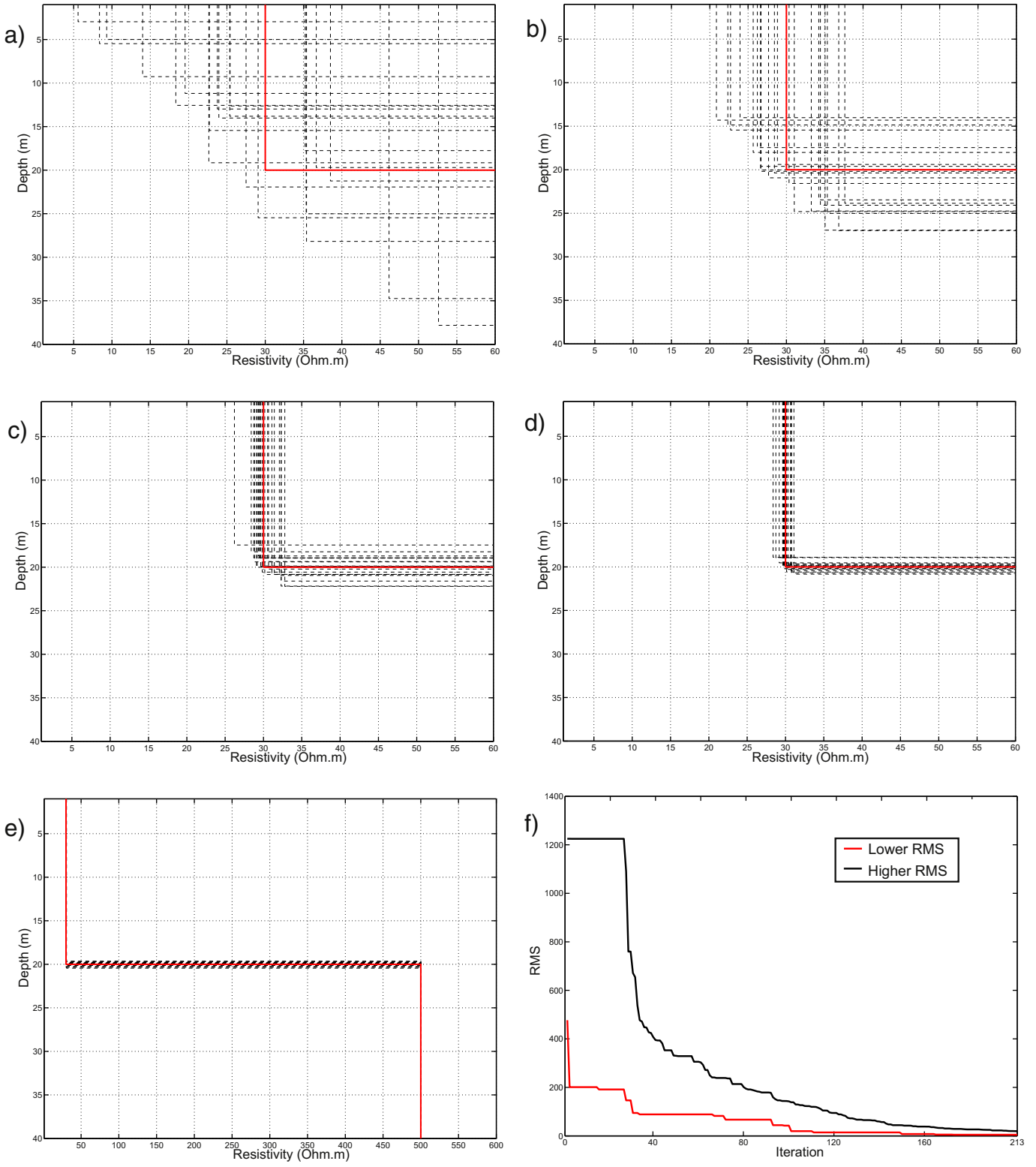

Fig. 4. Models used in CRS inversion in a geoelectric model representation. In a), b), c) and d) models in iterations 50, 100, 150, and 200 respectively, zoomed in the first layer (inversion parameters). In e) final figure generated by the program with the whole model represented (first and second layers). In f) lower and higher RMS of *m* set of models along the iterations are presented.

box. Fig. 3b shows models in the fiftieth iteration. In such a stage, models are now spread in search space, most of the models are out of initial search space, and models are searching the solution in the free space. Models are now mapping the objective function and the algorithm is selecting models close to local minimums and global minimum. Figs. 3c, d and e present iterations 100, 150 and 200. In this stage, models are approaching the solution and becoming close to each other. Models approach each other because they are now close to the solution (global minimum). This is how CRS avoid stop in local minimums, models will find the local minimums but eventually those that are close to global

minimum will stay there (lower RMS), and along iterations will bring others to the same region. Thus, global minimum is where most of models are in the final algorithm stage. Fig. 3f presents final models for iteration 213, with that one with lower RMS been the final inversion process model. As can be seen, CRS algorithm final set of models have ideally all models close to global minimum after enough iterations. In this case, the stop criterion was all models must have a RMS lower than 1%.

In Fig. 4, the representation of models in Fig. 3 is presented as geoelectric model. In Fig. 4a, b, c, and d, represented models are for iterations 50, 100, 150, and 200, respectively. These graphs are a more common way to represent a geoelectric model, in the same forms, it presents them in the program in here used. Fig. 4e presents the final geoelectric model for iteration 213. As previously described, all models tend to converge to global minimum and when plot together they overlaps each other. When result is overlapped models, for our case, the meaning is inversion was carried on with enough iterations and the result is reliable. Trying to calculate some statistics of final models may lead to some meaningless results, once it obtained these models, a tendentious way in algorithm. Fig. 4f presents the lower and higher RMS (in percentages) of m set of models along the iterations. It is possible to see the convergence to a good adjustment is done for the whole set; with a good number of iterations, models tend to converge to the global minimum. The first 30 iterations appears no change the higher RMS but changes occurs. It is not possible to see them very well because initially the changes are not significant enough to appear in this graph. After some tens of iterations, the changes are more evident. This pattern is present in several tests we completed.

A code called *Curupira* was developed in this research (Bortolozo and Porsani, 2012). The name is from a folkloric creature from Brazilian mythology, whose feet are inverted and who protects forests from destruction. The software is capable to make individual inversions of VES and TEM soundings (central-loop array) and to do the joint inversion of both data sets. It is also able to make the forward modeling of both methods by adding numerical noise (as describe early in this paper). The development of operational software seeks to make easier the inversion of soundings and puts the joint inversion available to more researchers. This software generated all results presented in this paper and was tested in many ways to assured its functioning and credibility.

2.4. Static shift correction

Meju (2005) presents empirical formulas in order to represent Vertical Electrical Sounding and TEM data in the same graph. It should emphasize that any kind of transformation is used. Formulas obtained by Meju (2005) are:

1. Representing Vertical Electrical Sounding in a time scale

$$t = \frac{\pi \mu_o \sigma L^2}{2} \tag{22}$$

where σ is the apparent conductivity for $AB/2 = L$.

2. Representing TEM soundings in AB/2 (meters) scale,

$$L = 711,8\sqrt{t\rho} \tag{23}$$

where ρ is the apparent resistivity in instant t.

Formulas are used in order to remove static shift that may be present in electrical surveys. VES curve may be static shifted because it has electrodes in contact with ground, and they are under the effect of heterogeneities in the fixed position. These heterogeneities may cause the existence of a secondary electrical field. This field causes the curve to move up or down parallel to apparent resistivity axis. The correction of static shift is required for proper inversion of combined data. The correction of static shift effect is done by multiplying the whole VES curve by a correction factor, so that the whole curve is shifted on y-axis (the axis of apparent resistivity) partially overlapping TEM curve. This procedure with real data is going to be demonstrated later in the paper.

3. Discussion of inversion results

3.1. Synthetic data

The joint inversion seeks for a better interpretation of underground by the combination of different databases. A better interpretation when compared with individual interpretation of different methods. Our goal is to map geoelectric stratigraphy of Bebedouro Region in Paraná Sedimentary Basin, in Brazil. In order to investigate the advantages of a joint inversion, a synthetic model that corresponds to real geoelectric stratigraphy observed in that area (Porsani et al., 2012b) was created. This synthetic model is represented in Fig. 5. Region geology will be further detailed in the text, but now we are going to take synthetic model. Initial layer of 8 m thick and 200 Ω.m resistivity represents a layer of unsatured soil/sediments. The second layer of resistivity 25 Ω.m and 55 m thick represents a saturated zone. The resistive layer below (800 Ω.m) 500 m thick represents a basaltic rock. The last layer represents Guarani Aquifer with 30-Ω.m sediment. This synthetic model is used in all tests of inversion, both in VES and TEM as well as VES/TEM 1D joint inversion. Results with synthetic data for the single VES inversion for the single TEM sounding inversion and VES/TEM 1D joint inversion are showed below. All inversions with synthetic data were done in the same conditions: same numbers of layers and same initial search space.

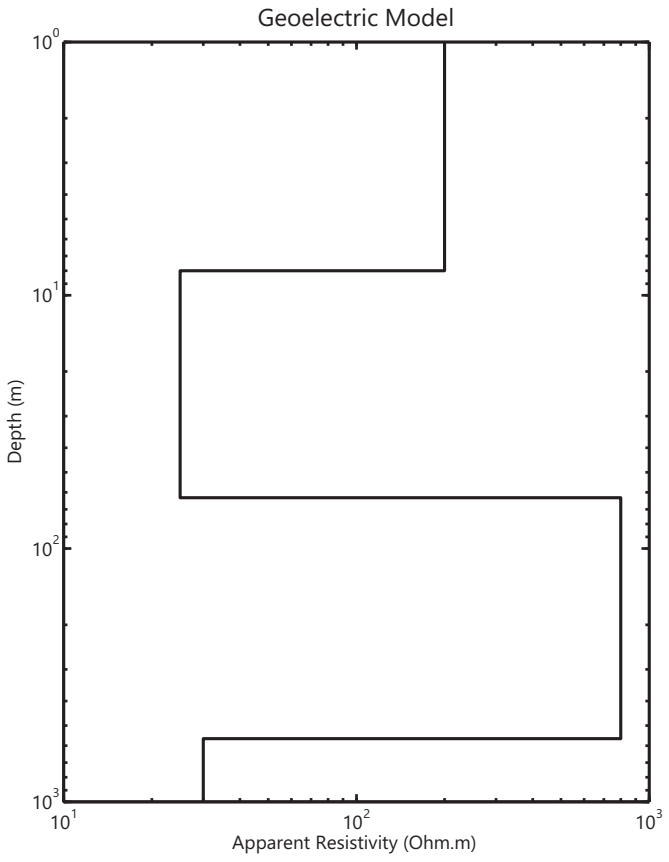

Fig. 5. Synthetic model based on geological information of Bebedouro region used in synthetic test.

To validate synthetic inversion, it is necessary to add numerical noise to synthetic data to simulate a real survey. Adding realistic noise can be a quite complex task. The most recommended way to have realistic noisy data is to make an interpretation of errors presented on real data and try to represent them numerically. For VES data, it considered noise is equally distributed but randomly throughout curve. The amplitude of noise varies (from zero to a maximum value) point to point. A maximum amplitude of noise was adopted, and a percentage as added or subtracted at each value of the curve. In this way, we simulate the normal variation in field data signal. In Fig. 6, synthetic curve with synthetic noise is compared to an experimental VES curve. It is possible to see small scattering in data that VES curves usually present. The error magnitude was determined from experimental data interpretation. The value of standard deviation obtained in our soundings in Bebedouro region was 0.42 Ω.m. Thus, the disturbance in data was gotten by adding or subtracting a percentage of three times of average standard deviation. The value of this percentage is random and different for each point.

Addition of artificial noise in TEM data was followed a quite different approach, due to the different pattern of the noise. Error distribution in TEM curve cannot be considered homogeneous. In the early times, error magnitude is very low, while the error amplitude is very large for latest times. The following equation calculated the noise:

$$\delta_{TDEM} = S\sqrt{-2\ln(r_1)}\ \cos(2\pi r_2)e^{-\left(\frac{(t_{max}-t)^2}{t}\right)} \quad (24)$$

where r_1 and r_2 are random numbers; S is the standard deviation; t_{max} is the last-time value of the curve; and t is the time value, corresponding to the time where noise is added. The calculation of standard deviation was based on real data. TEM equipment (PROTEM-57-MK2 — Geonics) used in the field work acquisition generates a file with three-curve resistivity values, corresponding to frequencies of repetition rate of 30 Hz, 7.5 Hz and 3 Hz. Then, we calculated the apparent resistivity standard deviation for each time, and the average standard deviation for each curve. Thus, it got standard deviation for each curve (three frequencies). Every sounding used this procedure, and the average deviation of all set of soundings was calculated reaching the value of 0.74 Ω.m. Fig. 7 shows synthetic noisy data compared to experimental data. As can be seen, the pattern of dispersion of synthetic noise is very close to the real.

Fig. 8 shows results for the single inversion of VES synthetic data. VES recovers well the first layer: its resistivity as well as its thickness. The second layer is also well solved. Third-layer top is at depth of 63 m, and its bottom is at 563 m depth. The maximum electrode spacing in the simulated VES is 400 m (AB/2 = 200 m). This corresponds to a maximum depth of investigation < 100 m deep. Therefore, it was expected that VES could not solve third-layer bottom as well as the deepest layer of 30 Ω.m of resistivity. Results show that VES can define the shallow layers but in the case of an electrode spacing of 400 m there is no capacity of investigate deep structures (below 100 m). In order to investigate structures deeper than 100 m, the electrode spacing must be increased. Nevertheless, this operation not always can be done in field-work. About the adjustment error, it is calculated as a percentage of data, i.e., the total error is given as a percentage of total data set value.

Fig. 9 shows results obtained from TEM sounding inversion. Shallow layer is not well solved. It expects this limitation because TEM sounding (central loop) cannot define with precision structures shallower than 10% the side of the transmitter loop. In addition, once the simulated loop has a side of 100 m, structures until 10 m depth cannot be solved. However, the deepest layers are quite well resolved. For instance, the second layer is very well resolved. The third layer has also a good resolution, although the inverted model overestimates this layer resistivity. Notwithstanding, this fact does not invalidate the inversion result. It might be noted geoelectric basement was determinate with precision in a simulated depth of 563 m.

Fig. 10 shows VES/TEM 1D joint inversion results, which illustrated that all model layers (Fig. 5) are well resolved. Shallow layers are very well solved, and the investigation depth now reaches geoelectric basement. It is possible to observe TEM inversion overestimated third-layer resistivity now with a value close to the "true" one. It also can be notice both data sets are fitted.

We do these tests to verify advantages of 1D joint inversion, and investigate how those advantages appear in inversion results. This procedure was crucial for our understanding of 1D joint inversion procedure and algorithm validation. After that, it inverted some other tests with synthetic data a pair of real soundings (VES/TEM).

3.2. Real data from Paraná Basin

After testing the potential of 1D joint inversion with synthetic data, we applied the developed program "*Curupira*" to invert real data. Used soundings were acquired in Paraná sedimentary basin, next to Bebedouro and Pirassununga cities. Bebedouro city is located in the north part of São Paulo State, in Brazil. Bebedouro region geology is characterized by a sedimentary package (Adamantina Formation) with thickness varying from 50 m to 100 m. There is a 500 m thick basalt layer (Serra Geral Formation) beneath sedimentary package. There is other sedimentary layer containing Guarani aquifer (Botucatu Formation) below basalts. According to deep wells information, the top of geological basement of Paraná Basin is between 2500 and 3000 m depth. The field setup was similar to that one used in synthetic tests: for VES a maximum value of AB/2 = 200 m was used, and a transmitter loop of 100 m × 100 m for TEM acquisition. In the region, there are many wells and some of them have available geological logging. Data from a well near to the survey (Fig. 11a) was used in geophysical model interpretation. Static shift correction was done, and

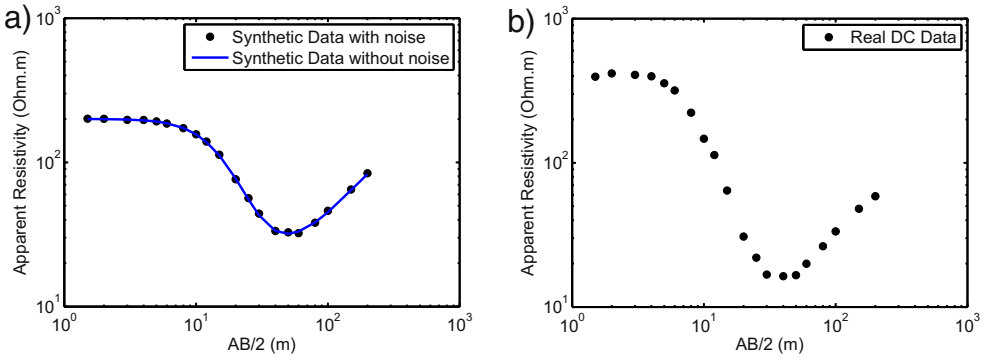

Fig. 6. VES synthetic sounding with numerical noise versus real VES: a) synthetic curve without noise (blue line), and synthetic curve with synthetic noise (black dots). b) Real VES curve. These figures show that the pattern of dispersion of synthetic noise is very close to the real one. (For interpretation of the references to color in this figure legend, the reader is referred to the web version of this article.)

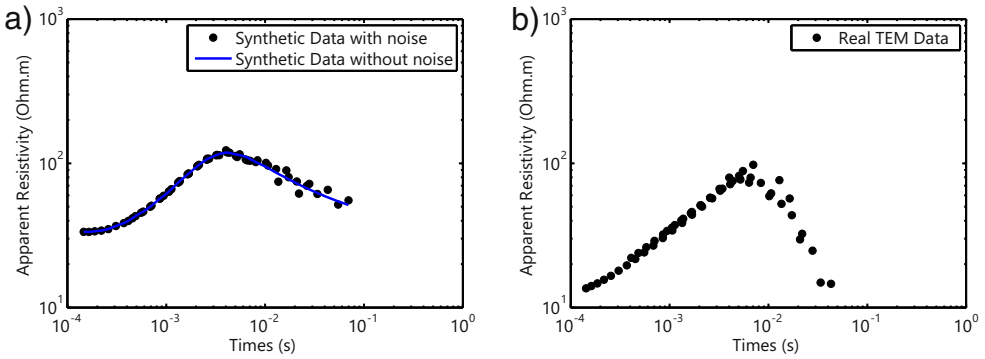

Fig. 7. TEM synthetic sounding with numerical noise versus real TEM: a) synthetic curve without noise (blue line), and synthetic curve with synthetic noise (black dots). b) Real TEM curve. These figures show that the pattern of dispersion of synthetic noise is very close to the real one. (For interpretation of the references to color in this figure legend, the reader is referred to the web version of this article.).

the result is showed in Fig. 12, the correction factor in this case was 0.88. Fig. 13 shows the inverted model for VES individual inversion. VES detect a few shallow layers. The first one, some-centimeter thick might correspond to superficial soil. The second layer with 4-meter thick corresponds to a dry sedimentary layer. The next downwards layer is conductive with a thickness of approximately 50 m, and may corresponds to a sedimentary aquifer present in the region. The deepest layer in VES model is a resistive layer (more than 400 Ω.m) corresponding to basalts of Serra Geral Formation.

Fig. 14 shows TEM individual inversion, which exemplifies the differences in both methods. TEM considered the upper layers as a single structure with 400 Ω.m of resistivity. The second layer corresponds to sedimentary aquifer present in the region. The third layer represents the basalts of the Serra Geral Formation. Actually, some distortion occurs in the depth of this layer top. The 20 m depth ascribed to this layer top does not match with borehole information in the area. The obtained inversion value is underestimated. This effect happens in some soundings in Bebedouro area, and it was associated to 2D structure presence (Almeida, 2011). This effect is very problematic and can generate some misunderstanding in the result interpretation. However, 2D does not seem to affect interferences at the bottom layer interpreted as Guarani aquifer in Botucatu Formation, and its depth and resistivity correspond to the observed in boreholes.

Fig. 15 shows VES/TEM 1D joint inversion results. VES individual inversion defines shallow layers, and TEM individual inversion reveals the deepest layer. TEM individual inversion underestimates the depth of third-layer top that is now in agreement with borehole information of the area. As in TEM inversion, the result with 1D joint inversion indicates that the bottom layer at almost 700 m depth. Cleary, results show that 1D joint inversion obtains the best of both methods. In Fig. 16 we present a geoelectric profile in Bebedouro city. The profile goes from southwest to northeast, and we can see the basalt thickness variation. Between soundings T75, T76, T77, the depth of basalt base are practically the same as well as between soundings T78, T79, T80, T81, and T82. However, in soundings T77 and T78 there is a great difference between the depths of basalt base suggesting to be a geological structure. Almeida (2011) as well Porsani et al. (2012b) well described this geoelectric structures detected with VES and TEM.

A second joint inversion example was performed by using data obtained next to Pirassununga city, also locate in São Paulo State. The

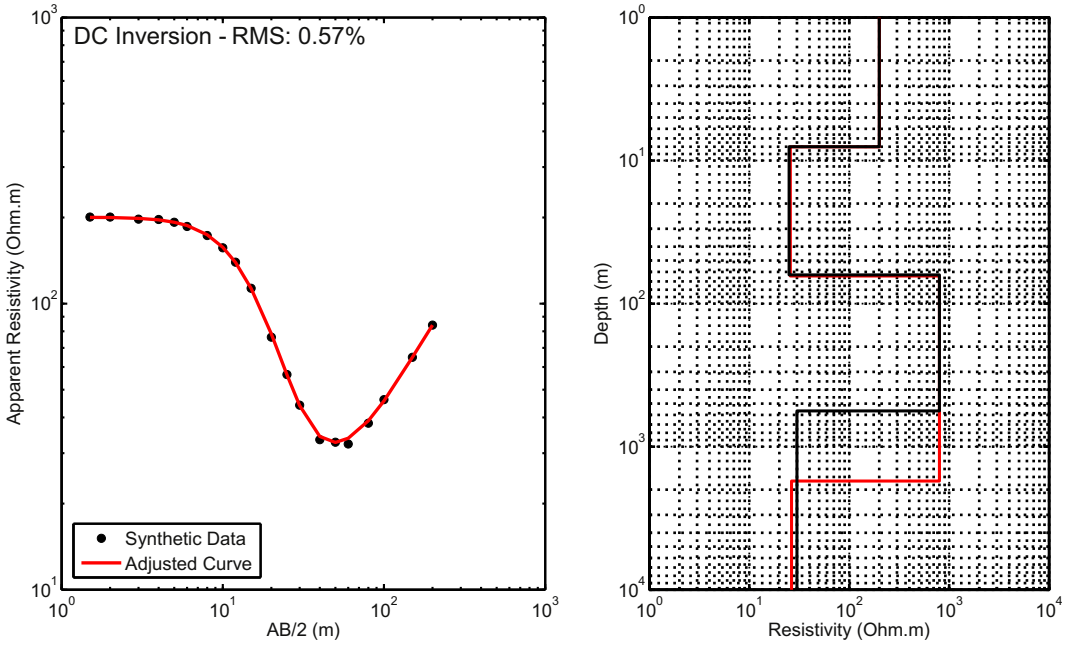

Fig. 8. Inversion results of VES Synthetic data with noise. a) Synthetic curve with inverted curve adjusted. b) Inverted geoelectric model (black line) compared with real model (red line). (For interpretation of the references to color in this figure legend, the reader is referred to the web version of this article.)

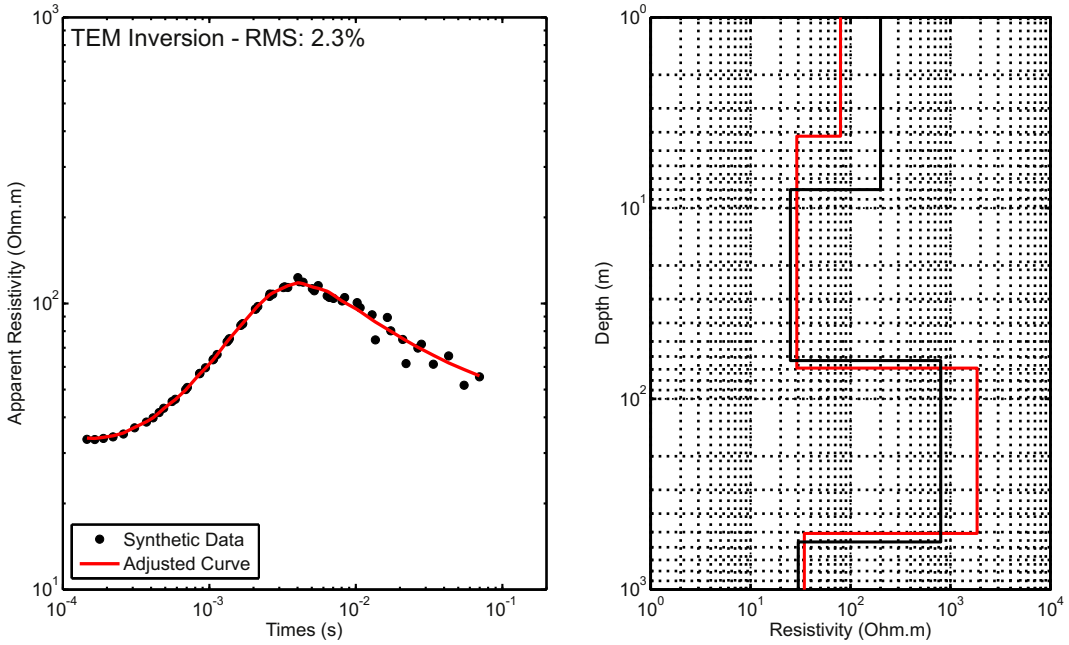

Fig. 9. Inversion results of TEM Synthetic data with noise. a) Synthetic curve with inverted curve adjusted. b) Inverted geoelectric model (black line) compared with real model (red line). (For interpretation of the references to color in this figure legend, the reader is referred to the web version of this article.)

survey is located inside USP (*Universidade de São Paulo*) campus. The location is ideal for TEM soundings, once there are neither urban noises nor coupling effects. The main target for this research in Pirassununga was to define the top and base of diabase intrusion present in the area for hydrogeological purpose.

Massoli (1983) described geological sketch of study area and it corresponds to Cenozoic's sediments (sand) of Pirassununga Formation covering claystones of Corumbataí Formation. Under claystones is diabase intrusion (Serra Geral Formation) with a variable thickness. Iratí Formation, composed of shales, is present under diabase intrusion.

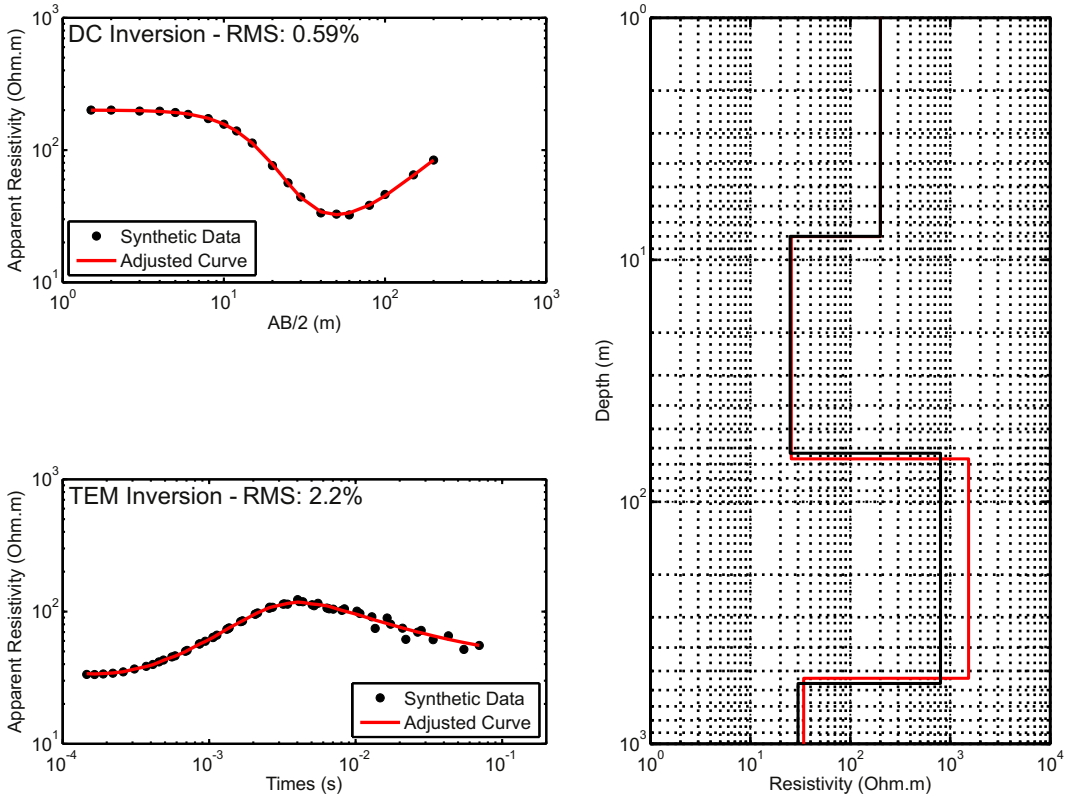

Fig. 10. Synthetic VES/TEM 1D joint inversion results. a) Synthetic VES curve with inverted curve adjusted. b) Synthetic TEM curve with inverted curve adjusted. c) Inverted geoelectric model (black line) compared with real model (red line). (For interpretation of the references to color in this figure legend, the reader is referred to the web version of this article.)

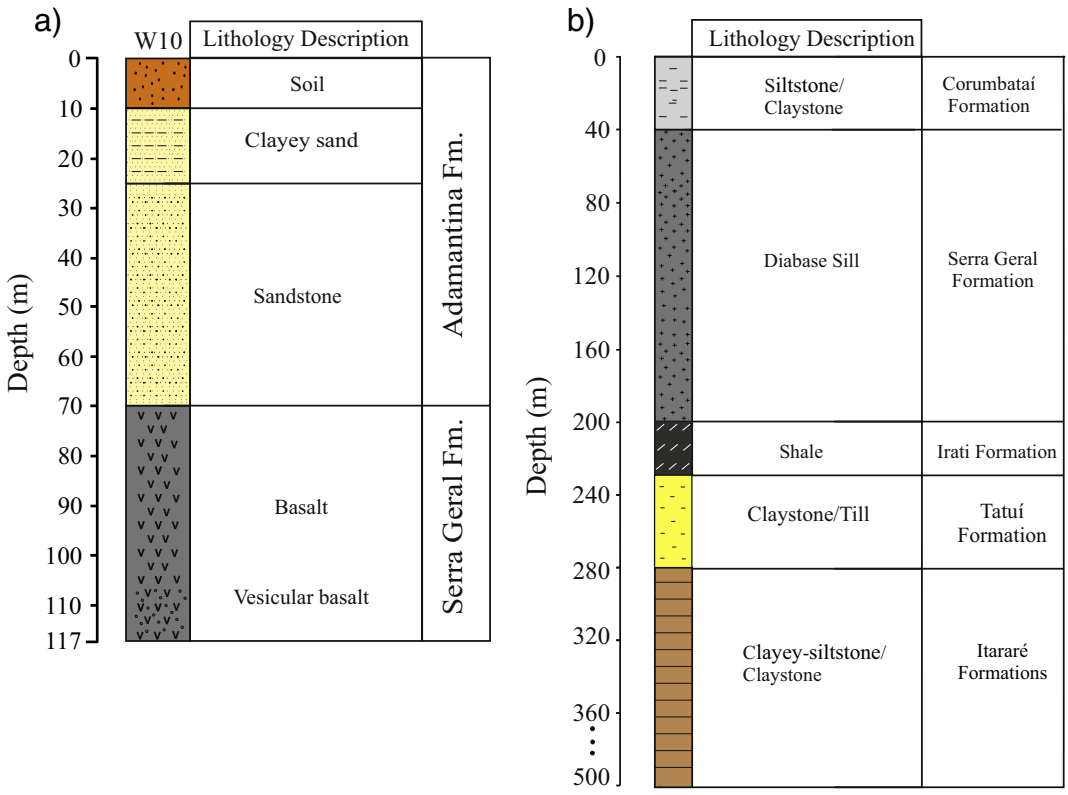

Fig. 11. Representation of borehole lithological information. a) Lithological information of Bebedouro region. b) Lithological information of Pirassununga region.

Tubarão Super Group that comprises Tatuí and Itararé Formations is below Iratí Formation. Tatuí Formation is mainly composed of intercalated clayey-siltstones and claystones. On the other hand, Itararé Formation is composed of sandstones, tills, conglomerate, and claystones. Obtaining borehole information was from a water supply well drilled in the surrounding area after doing soundings, and Fig. 11b shows it.

Fig. 17 shows VES data individual inversion. As in Bebedouro case, VES solves the shallowest soil layers and initial sedimentary pack until ~2 m depth. This initial sedimentary pack is Cenozoic's sediments of Pirassununga Formation. The layer between 2 m and 20 m is probably Corumbataí Formation claystone. The third layer is diabase sill that was the main survey target. Sill has about 41 m thick and almost reaches

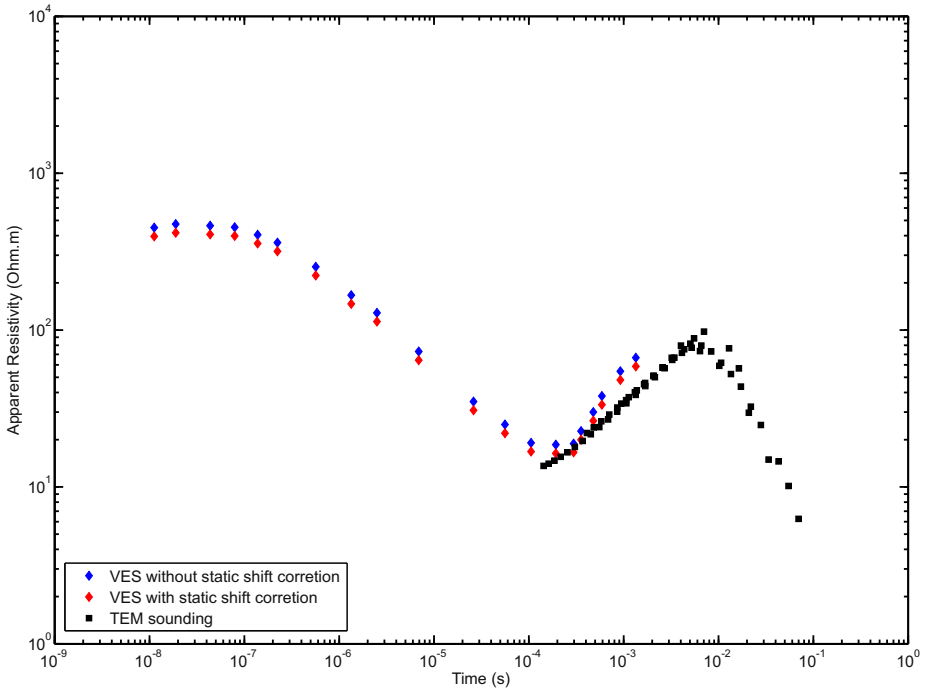

Fig. 12. Static shift correction for Bebedouro VES sounding.

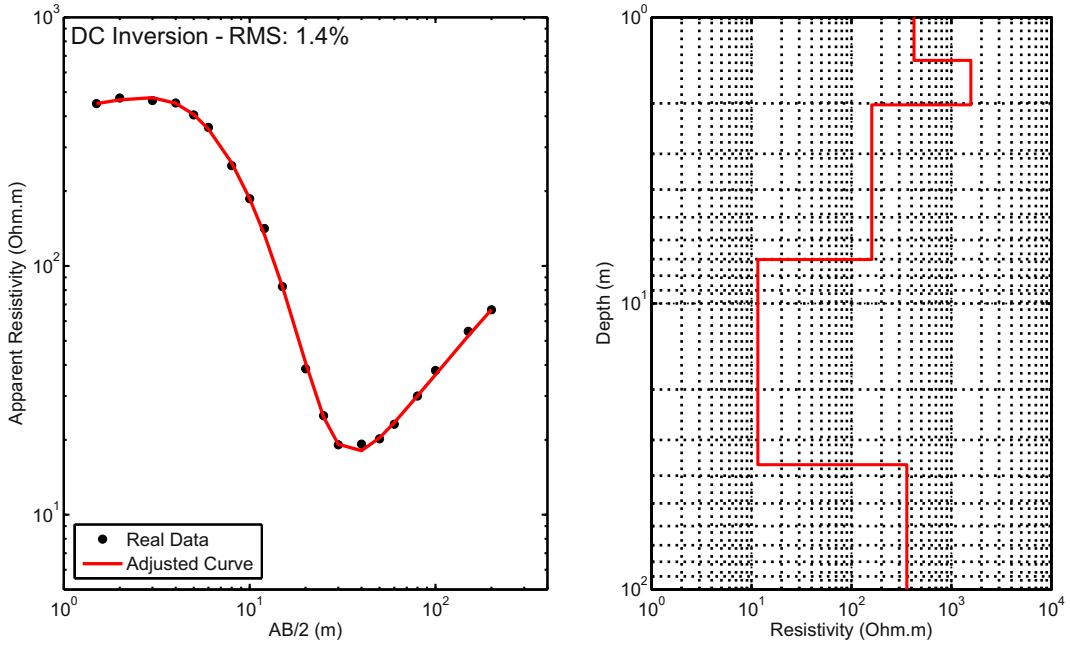

Fig. 13. Results of Bebedouro VES inversion. a) Real VES curve with inverted curve adjusted. b) Inverted geoelectric model.

63 m depth. Beneath sill there is a conductive layer, which was at first assumed to correspond to Tatuí Formation or Irati Formation. However, with a more accurate interpretation was realize that it probably corresponds to a fractured zone in diabase sill that continues after fractured zone.

TEM inversion (Fig. 18) could not define the shallowest layers, being incapable to define Corumbataí Formation. Nevertheless, the top and base of basaltic intrusion was marked and TEM sounding reached more deep layers. VES could not precisely define conductive layer under the sill. Moreover, with the TEM sounding was possible to estimate the thickness of diabase intrusion, that corresponds to the resistive layer starting in 20 m depth, goes to the 60 m thick conductive layer that begins in 90 m depth and ends with the other resistive layer that goes until 230 m depth. Then, with TEM sounding the total thickness of the sill is around 209 m, including the first resistive layer, fractured zone (also detected with VES) and the other resistive layer. The deepest layer detect by TEM sounding probably corresponds to the sedimentary package formed by shales of Iratí Formation and sediments of Tubarão Super Group (Tatuí and Itararé Formations). TEM method could not precisely define contacts among these sedimentary packages probably due to the lack of resistivity contrast and loss of resolution in deep.

After static shift correction (Fig. 19) the joint inversion was accomplished. In such a case, the correction factor used was 5. Fig. 20 shows the results. Once again, the joint inversion brings the best of both methods into a single model that has all layers presented in VES and TEM inversions. The same geoelectric model could define the top of

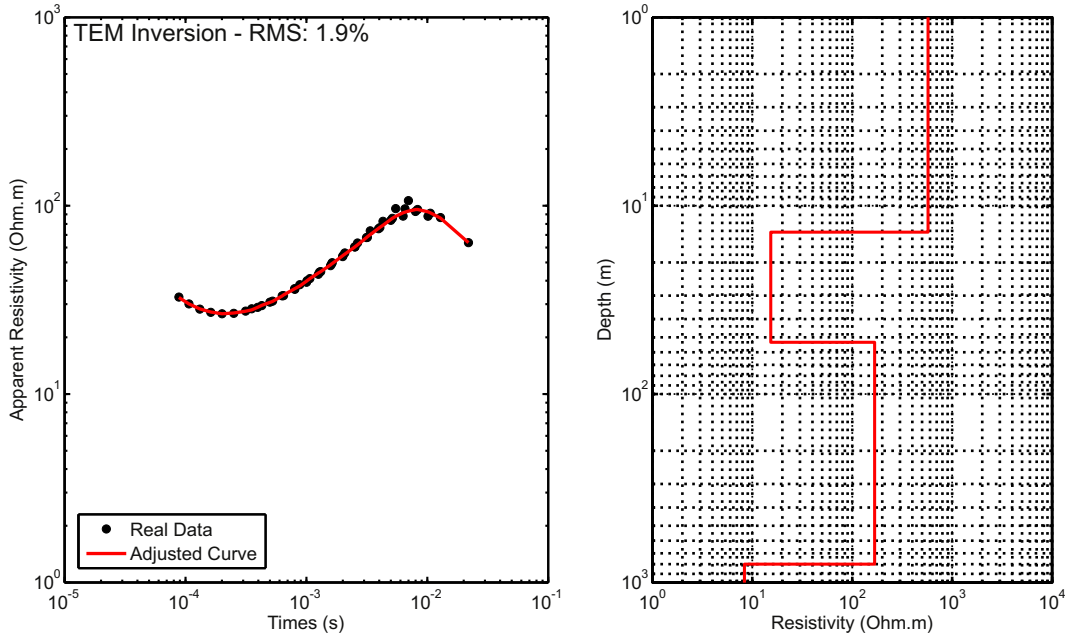

Fig. 14. Results of Bebedouro TEM inversion. a) Real TEM curve with inverted curve adjusted. b) Inverted geoelectric model.

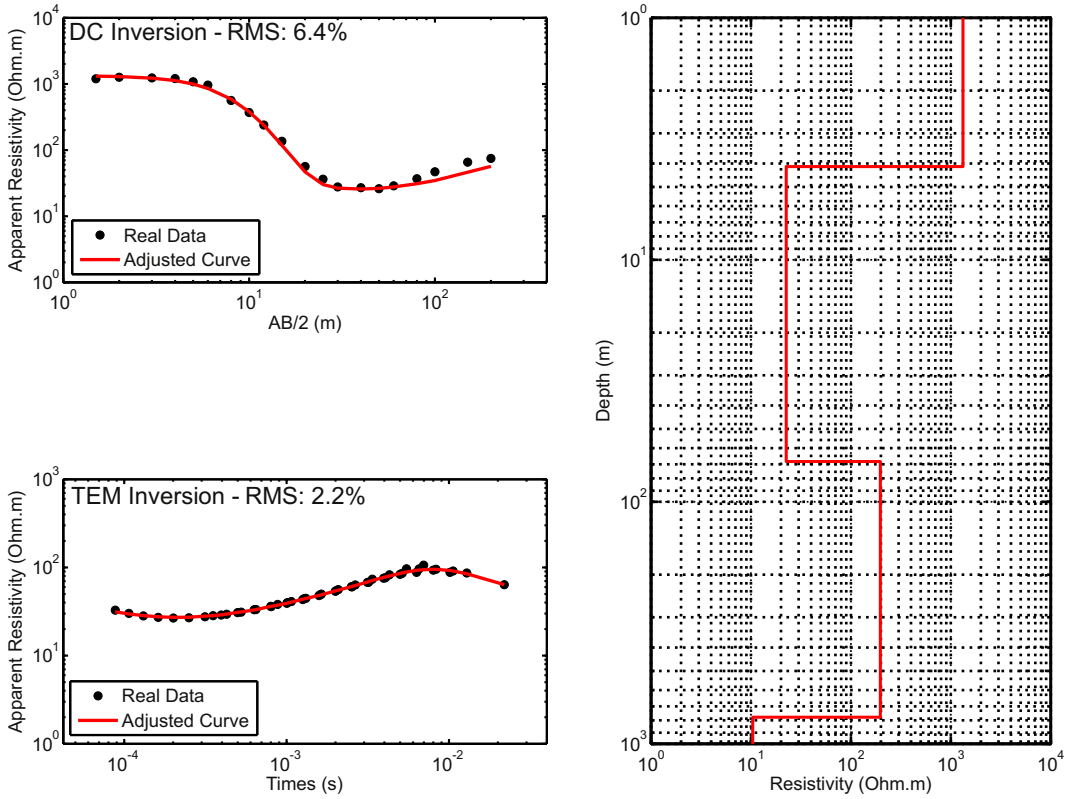

Fig. 15. Results of Bebedouro VES/TEM 1D joint inversion. a) Real VES curve with inverted curve adjusted. b) Real TEM curve with inverted curve adjusted. c) Inverted geoelectric model.

diabase intrusion as revealed in VES and TEM soundings and the layer deeper than 200 m was also reach as in TEM sounding. The main difference from the individual and joint inversions in the Pirassununga case is the advantage of having one single model that adjust the both curves and reaches all the layers detected in the individual sounding. The shallow layers detect in VES and the deepest ones reach by TEM are all in one single model. Once in Pirassununga VES sounding the static shift was much higher than in Bebedouro case, we try to make the 1D joint inversion without the static shift correction. Fig. 21 presents VES and TEM 1D joint inversion without VES static shift correction. In this view, TEM data adjustment is worst than with static shift correction. Inverted model is considerable different from the one obtained with static shift correction.

Inverted models in Figs. 20 and 21 are similar in means of number of layers and resistivity contrasts. However, layer interfaces are considerable different. Besides, the model in Fig. 21 tends to have more resistive

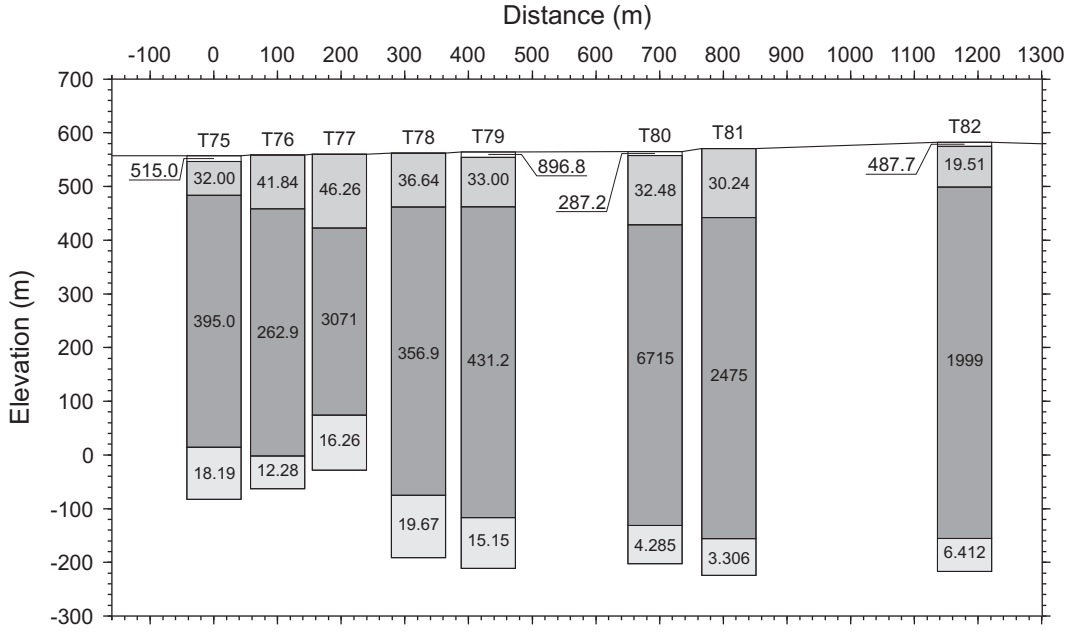

Fig. 16. Geoelectrical profile, generated by contouring 8 TEM soundings located in Bebedouro area showing the formation resistivity *vs.* elevation.

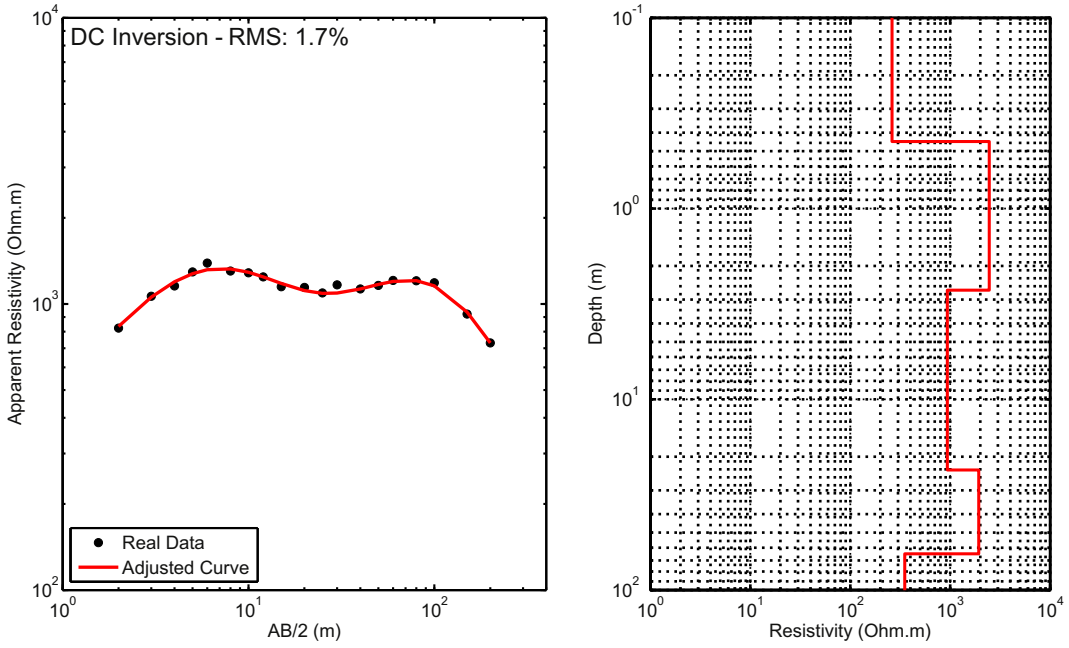

Fig. 17. Results of Pirassununga VES inversion. a) Real VES curve with inverted curve adjusted. b) Inverted geoelectric model.

layers. Models diverge about layer interfaces, making this the major difference between these models. Once static shift correction puts database in a closing resistivity range, this can give more reliable as well less ambiguous result. As presented in these examples, 1D joint inversion without static shift correction is possible but not recommended.

4. Conclusions

In this paper we presented a methodology for 1D joint inversion of VES and TEM data by using CRS algorithm. Results clearly showed that the joint inversion puts together the best advantages of both methods. In our case, VES gives information to determine accurately the shallow layers, while TEM soundings provided information until about 900 m depth. The use of two methods with different sensitivities to noise and distortion effects allows improving the reliability of the results, once distortions affecting one of the methods possibly will not affect the other, as in Bebedouro case. In Pirassununga case 1D joint inversion showed how the final study result is improved, demonstrating this methodology is a powerful tool for electromagnetic methods.

Data acquisition for 1D joint inversion is easily performed. The only recommendation is that surveys should have the centers as close as possible, because local resistivity variations can differently influence data. Another important step is static shift correction using Meju's equations as previously described. This procedure will ensure more accurate results once inverted model will be able to adjust both curves without any trouble related to disturbing scale effects in VES curves. Besides, this procedure is easily completed, even with worksheet softwares being not a major issue.

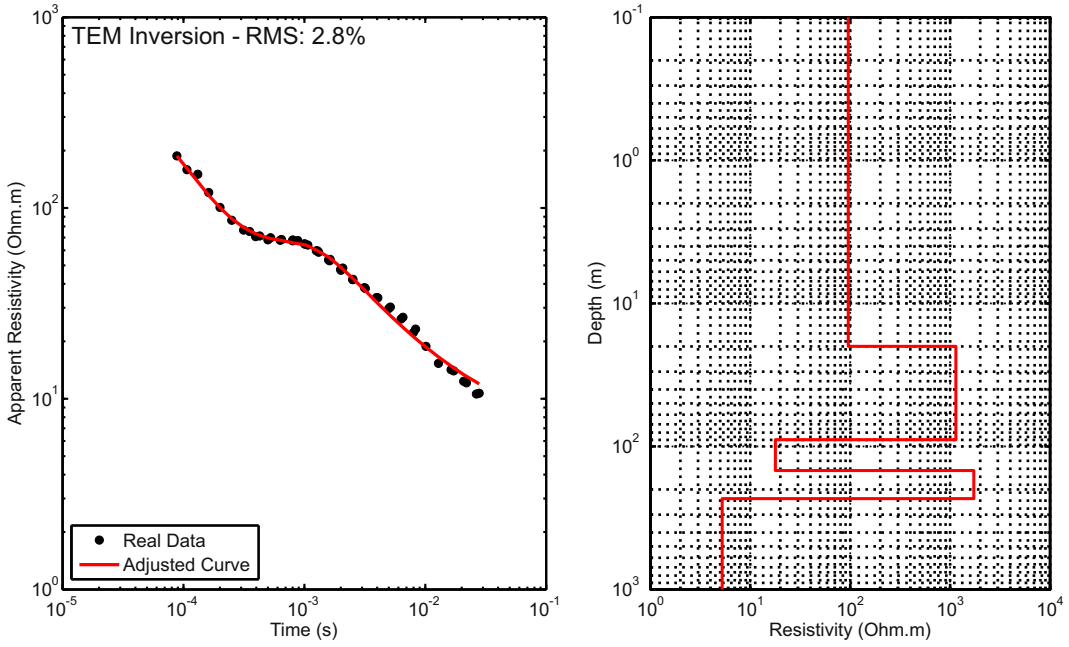

Fig. 18. Results of Pirassununga TEM inversion. a) Real TEM curve with inverted curve adjusted. b) Inverted geoelectric model.

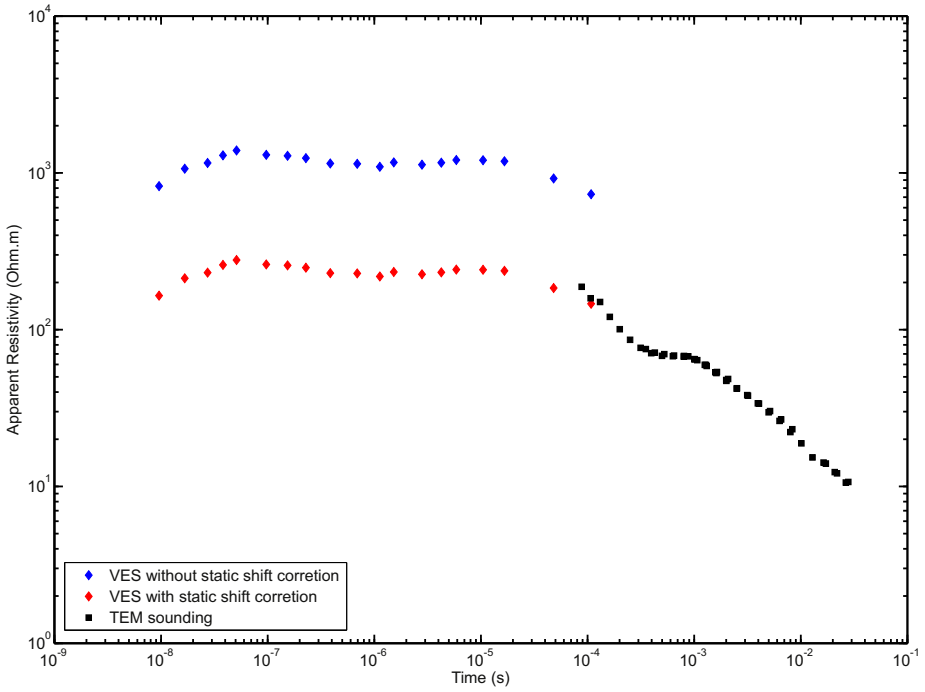

Fig. 19. Static shift correction for Pirassununga VES sounding.

In this paper we present inversions obtained by CRS algorithm. In the literature, global search algorithms are used in many cases but especially with TEM and TEM and VES 1D joint inversion these algorithms are fairly used. Here we presented some interesting results for these cases. Demonstrating that global search algorithms can be reliably used with respect to computation time in modern computers for 1D problems. The major advantages of global search are that it drastically reduces the chance to stop in local minimums and presents the robustness to deal with two data sets in a joint inversion.

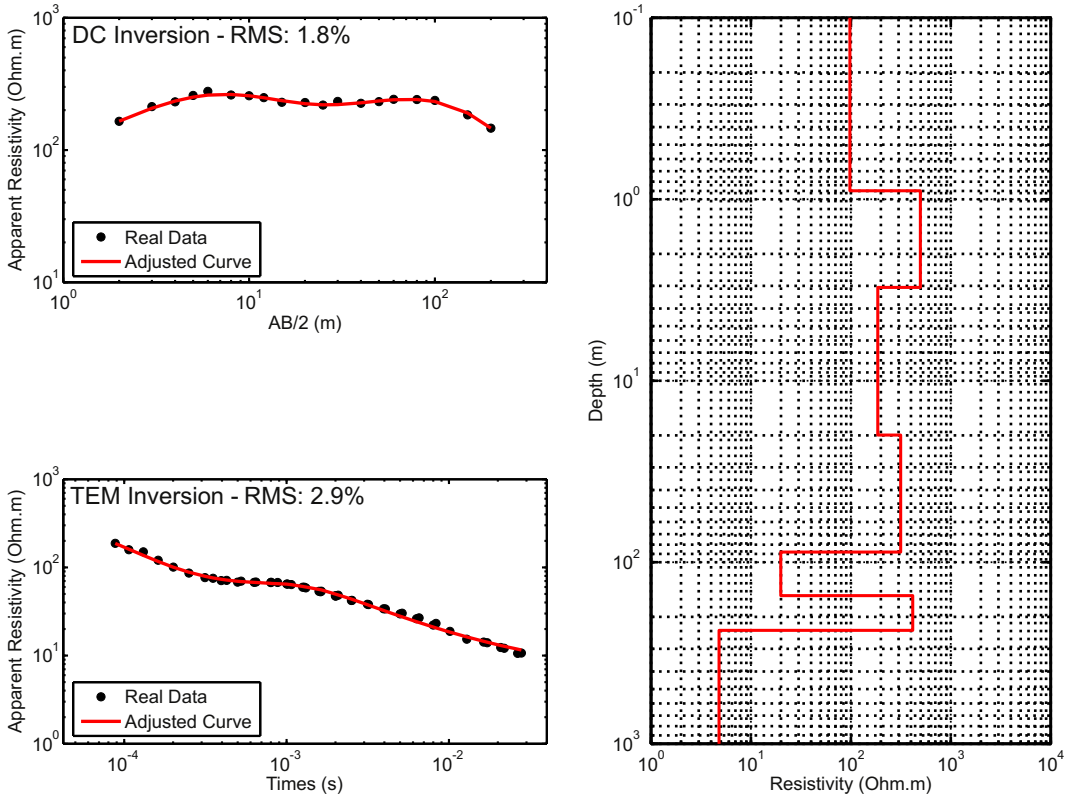

Fig. 20. Results of Pirassununga VES/TEM 1D joint inversion, with VES static shift correction. a) Real VES curve with inverted curve adjusted. b) Real TEM curve with inverted curve adjusted. b) Inverted geoelectric model.

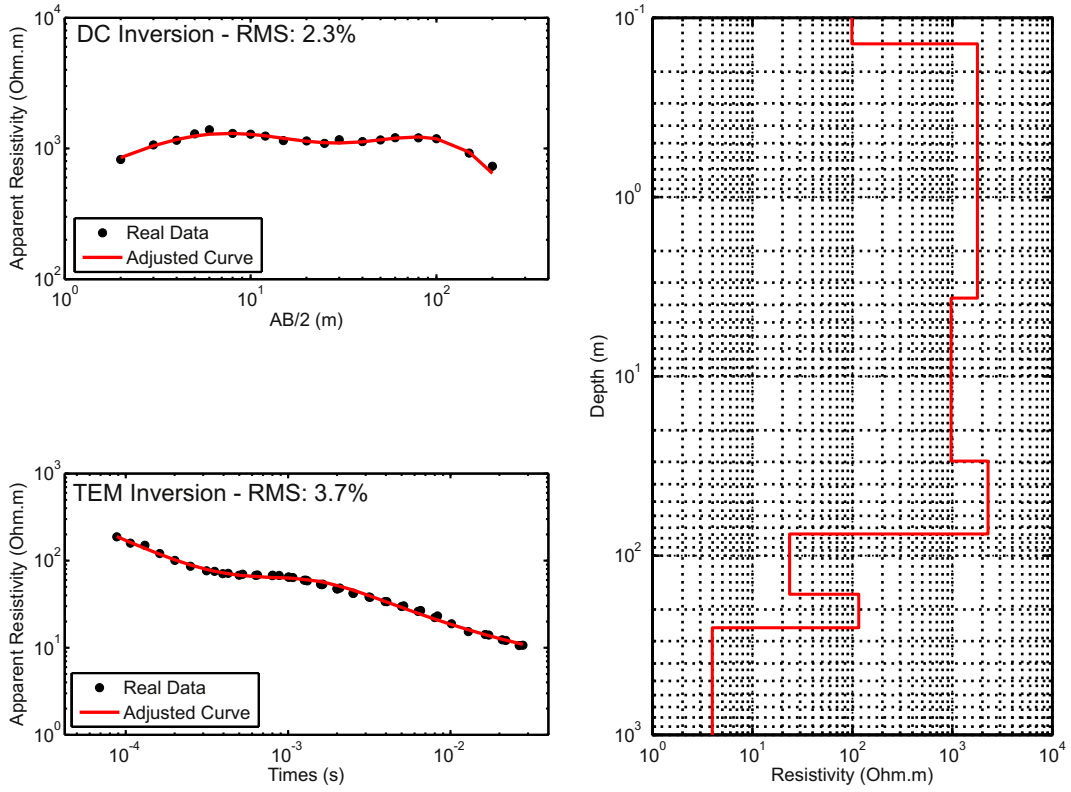

Fig. 21. Results of Pirassununga VES/TEM 1D joint inversion, without VES static shift correction. a) Real VES curve with inverted curve adjusted. b) Real TEM curve with inverted curve adjusted. b) Inverted geoelectric model.

Acknowledgments

CAB acknowledges *Coordenação de Apoio à Pesquisa de Ensino Superior* (CAPES) for providing a fellowship. JLP acknowledges *Fundação de Amparo à Pesquisa do Estado de São Paulo* (FAPESP) for providing financial support to this research (Grants 2009/08466-3 and 2012/15338-4). Both CAPES and FAPESP are Brazilian research agencies. We thank IAG/USP for providing infrastructure support. We also thank Ernande, Vinícius, Marcelo, David, Divanir, Thiago, and other students for helping in geophysical data acquisition.

References

Albouy, Y., Andrieux, P., Rakotondrasoa, G., Ritz, M., Descloitres, M., Join, J.L., Rasolomanana, E., 2001. Mapping coastal aquifers by joint inversion of DC and TEM soundings—three case histories. Ground Water 39 (1), 87–97.

Almeida, E.R., 2011. Caracterização geoelétrica na região de Bebedouro-SP por meio de sondagens eletromagnéticas no domínio do tempo (TDEM). Master Science, Departamento de Geofísica, Instituto de Astronomia, Geofísica e Ciências Atmosféricas, University of São Paulo, p. 158.

Bortolozo, C.A., Porsani, J.L., 2012. "CURUPIRA V1.0". Software de inversão conjunta 1D de sondagens SEV/TDEM. Registro de Programa de Computador no. 12988-1. Revista da Propriedade Industrial 2165, 145 (item 090).

Bortolozo, C.A., Couto Jr., M.A., Porsani, J.L., Almeida, E.R., Monteiro Santos, F.A., 2014. Geoelectrical characterization using joint inversion of VES/TEM data: a case study in Paraná Sedimentary Basin, São Paulo State, Brazil. J. Appl. Geophys. 111, 33–46.

Carrasquila, A.A.G., Ulugergerli, E., 2006. Evaluation of the transient electromagnetic geophysical method for stratigraphic mapping and hydrogeological delineation in campos basin, Brazil. Rev. Bras. Geofís. 24, 333–341.

Červ, V., Menvielle, M., Pek, J., 2007. Stochastic interpretation of magnetotelluric data, comparison of methods. Ann. Geophys. 50, 1.

Christensen, N.B., 1990. Optimized fast Hankel transform filters. Geophys. Prospect. 38 (5), 545–568.

Ghosh, D.P., 1971a. The application of linear filter theory to the direct interpretation of geoelectrical resistivity sounding measurements. Geophys. Prospect. 19 (1), 192–217.

Ghosh, D.P., 1971b. Inverse filter coefficients for the computation of apparent resistivity standard curves for a horizontally stratified earth. Geophys. Prospect. 19 (4), 769–775.

Goldberg, D.E., 1989. Genetic Algorithms in Search, Optimization and Machine Learning. Addison-Wesley Longman Publishing.

Goldman, M., Du Plooy, A., Eckard, M., 1994. On reducing ambiguity in the interpretation of transient electromagnetic sounding data. Geophys. Prospect. 42, 3–25.

Johansen, H.K., 1975. An interactive computer/graphic-display-terminal system for interpretation of resistivity sounding. Geophys. Prospect. 23, 449–450.

Kim, D., Kang, M., Rhee, S., 2005. Determination of optimal welding conditions with a controlled random search procedure. Weld. J. 8, 125-s.

Koefoed, O., 1970. A fast method for determining the layer distribution from the raised kernel function in geoelectrical sounding. Geophys. Prospect. 18, 564–570.

Koefoed, O., 1972. A note on the linear filter method of interpreting resistivity sounding data. Geophys. Prospect. 20, 403–405.

Křivý, I., Tvrdík, J., 1995. The controlled random search algorithm in optimizing regression models. Stat. Softw. Newsl. 20, 199–204.

Křivý, I., Tvrdík, J., Krpec, R., 2000. Stochastic algorithms in nonlinear regression. Comput. Stat. Data Anal. 33, 277–290.

Massoli, M., 1983. Geologia da folha de Piraçununga, SP. Rev. Inst. Geol. 4 (1–2), 25–51.

Meju, M.A., 1996. Joint inversion of TEM and distorted MT soundings: some effective practical considerations. Geophysics 61 (1), 56–65.

Meju, M.A., 2005. Simple relative space-time scaling of electrical and electromagnetic depth sounding arrays: implications for electrical static shift removal and joint DC-TEM data inversion with the most-squares criterion. Geophys. Prospect. 53, 1–17.

Merad, L., Bendimerad, F., Meriah, S.M., 2006. Controlled random search optimization for linear antenna arrays. Radio Eng. 15, 3.

Monteiro Santos, F.A., El-Kaliouby, H., 2010. Comparative study of local versus global methods for 1D joint inversion of direct current resistivity and time-domain electromagnetic data. Near Surf. Geophys. 8, 135–143.

Mosegaard, K., Sambridge, M., 2002. Monte Carlo analysis of inverse problems. Inverse Probl. 18, R29–R54.

Mosegaard, K., Tarantola, A., 1995. Monte Carlo sampling of solutions to inverse problems. J. Geophys. Res. Solid Earth 100, 12431–12447.

Nielsen, T.I., Baumgartner, F., 2006. CR1Dmod: a Matlab program to model 1D complex resistivity effects in electrical and electromagnetic surveys. Comput. Geosci. 32 (9), 1411–1419.

Porsani, J.L., Bortolozo, C.A., Almeida, E.R., Santos Sobrinho, E.N., Santos, T.G., 2012a. TDEM survey in urban environmental for hydrogeological study at USP campus in São Paulo city, Brazil. J. Appl. Geophys. 76, 102–108.

Porsani, J.L., Almeida, E.R., Bortolozo, C.A., Monteiro Santos, F.A., 2012b. TDEM survey in an area of seismicity induced by water wells in Paraná sedimentary basin, Northern São Paulo State, Brazil. J. Appl. Geophys. 80, 1–9.

Price, W.L., 1977. A controlled random search procedure for global optimization. Comput. J. 20, 367–370.

Raiche, A.P., Jupp, D.L.B., Rutter, H., Vozoff, K., 1985. The joint use of coincident loop transient electromagnetic and Schlumberger sounding to resolve layered structures. Geophysics 50, 1618–1627.

Sambridge, M., 1999a. Geophysical inversion with a neighbourhood algorithm — I. Searching a parameter space. Geophys. J. Int. 138, 479–494.
Sambridge, M., 1999b. Geophysical inversion with a neighbourhood algorithm — II. Appraising the ensemble. Geophys. J. Int. 138, 479–494.
Schmutz, M., Albouy, Y., Guerin, R., Maquaire, O., Vassal, J., Schott, J.J., Descloitres, M., 2000. Joint electrical and time domain electromagnetism (TDEM) data inversion applied to the Super Sauze earthflow (France). Surv. Geophys. 21, 371–390.
Schmutz, M., Guérin, R., Andrieux, P., Maquaire, O., 2009. Determination of the 3D structure of an earthflow by geophysical methods: the case of Super Sauze, in the French southern Alps. J. Appl. Geophys. 68, 500–507.
Sen, M., Stoffa, P., 1991. Nonlinear one-dimensional seismic waveform inversion using simulated annealing. Geophysics 56 (10), 1624–1638.
Silva, J.B.C., Hohmann, G.W., 1983. Nonlinear magnetic inversion using a random search method. Geophysics 48 (12), 1645–1658.
Smith, D.N., Ferguson, J.F., 2000. Constrained inversion of seismic refraction data using the controlled random search. Geophysics 65 (5), 1622–1630.
Vozoff, K., Jupp, D.L.B., 1975. Joint inversion of geophysical data. Geophys. J. Int. 42, 977–991.
Yang, C.H., Tong, L.T., 1999. A study of joint inversion of direct current resistivity, transient electromagnetic and magnetotelluric sounding data. Terr. Atmos. Ocean. Sci. 10, 293–301.